Electrochemistry of Cytochrome c_4 from *Pseudomonas stutzeri*

Jens-J. Karlsson,[†] Merete F. Nielsen,[‡] Marianne H. Thuesen,[†] and Jens Ulstrup*,[†]

Department of Chemistry, Building 207, Technical University of Denmark, DK-2800 Lyngby, Denmark, and Department of Chemistry, Symbion Science Park, University of Copenhagen, Fruebjergvej 3, DK-2100 Copenhagen Ø, Denmark

Received: September 6, 1996; In Final Form: December 27, 1996[⊗]

The cyclic voltammetry of the dipolar, overall negatively charged bacterial di-heme protein cytochrome c_4 from *Pseudomonas stutzeri* is composite and shows nontraditional features. Close to reversible voltammetry, with individual peaks corresponding to electron exchange of each heme, is found at high ionic strength (0.1 M phosphate, pH = 7.5) using gold electrodes modified by any of the promoters 4,4′-bipyridyl disulfide (4,4′-bpySS), 2,2′-dithiobisethaneamine (cystamine), and 3-pyridinylmethylenehydrazine carbothiamide. These are otherwise known to promote electrochemistry of proteins with positive, negative, and either positive or negative overall charges, respectively. This observation is indicative of weak surface orientational selectivity of cyt c_4 at high ionic strength. In contrast, the voltammograms at low ionic strength (0.01 M phosphate, pH = 7.5) point toward orientational selectivity in accord with the expected charge compatibility of the promoters with given domains of the protein. Numerical analysis of the voltammograms provide first macroscopic midpoint potentials and interfacial electron-transfer (ET) rate constants of each heme. The midpoint potentials at high buffer concentration are close to values previously determined from ET kinetics in homogeneous solution. At low ionic strength where orientational selectivity at 4,4′-bpySS- and cystamine-modified electrodes is likely, intramolecular ET between the heme groups is, secondly, a feature of the overall interfacial kinetics. The intramolecular rate constants can be determined from the voltammetric peak shapes, giving 40 s^{-1} for ET from the high- to the low-potential heme and 1600 s^{-1} for the reverse reaction. These values hold interesting implications in relation to the electronic structure and ET patterns in homogeneous solution.

Introduction

Well-behaved electrochemistry of small redox proteins has been achieved almost as a routine matter over the last decade.[1−6] Characterization of multicenter redox proteins is less straightforward due to composite voltammetry and interactions between the centers. Two-center redox proteins represent interesting intermediate patterns. On one hand their electron-transfer (ET) behavior is composite,[7−9] including cooperative effects, but the overall pattern is less entangled than for larger multicenter enzymes and offer prospects for more complete kinetic resolution. Cytochromes c_4 are interesting in this respect.[9−21] These are bacterial di-heme proteins and represent the simplest form of a multicenter protein. Their reduction potentials are indicative of biological function close to terminal oxidases[11,12,14] and well enough separated that individual heme characterization is feasible.

Pseudomonas stutzeri cytochrome c_4 is a well-characterized representative of this class. The primary[19] and three-dimensional structures[20,21] have recently been determined. The protein consists of two domains, each holding a single heme group. The domains are connected by a single polypeptide chain and an extended hydrogen-bond network. The overall charge of the protein moiety is −3 at neutral pH, but the charge distribution is asymmetrical with an excess of one positively charged amino acid in the C-terminal domain and four negatively charged amino acids in the N-terminal domain. NMR, resonance Raman and UV/VIS spectral characterization,[22] and kinetic ET resolution[9,10] have also become available.[22] The macroscopic reduction potentials of the hemes have finally been determined as 241 and 328 mV (SHE)[9] and represent interesting combinations of microscopic potentials and inter-heme interactions.

A key issue has been to disentangle the inter- and intramolecular ET schemes. Previous approaches include stopped-flow[9,10,15] and NMR spectroscopy[22] where no intramolecular ET has been directly detected. This implies that intramolecular ET must either be faster or slower than the millisecond time scale. Cyclic voltammetry offers an interesting alternative, rooted in the dipolar nature of cyt c_4. It could be anticipated that protein orientation at the electrode surface could be controlled by promoter molecules known to activate specifically *either* positively *or* negatively charged proteins[1−4,23,24] and *imposing* intramolecular ET in the overall electrochemical process. We present here cyclic voltammetric investigations of *P. stutzeri* cyt c_4 at modified gold electrodes. The voltammograms do follow simple association modes in which intramolecular ET is likely. The results are of interest for several reasons: First, dynamic electrochemical investigations of cyt c_4 have not been reported before. Second, voltammetry was obtained for cyt c_4 at gold electrodes modified with the three promoters 2,2′-dithiobisethanamine (cystamine), 4,4′-bipyridyl disulfide (4,4′-bpySS), and 3-(pyridinylmethylene)hydrazine carbothioamide (3-PMHC). The first two promoters are known to promote electrochemistry *exclusively* of negatively and positively charged proteins,[3,23,24] respectively, whereas 3-PMHC is a promoter for *either* positively or negatively charged proteins.[23,24] Third, intramolecular ET between the hemes is a crucial prerequisite that interfacial cyt c_4 ET can occur. Numerical simulation of the voltammograms provides an estimation of the intramolecular ET rate constants.

[†] Technical University of Denmark.
[‡] University of Copenhagen.
[⊗] Abstract published in *Advance ACS Abstracts,* March 1, 1997.

S1089-5647(96)02725-3 CCC: $14.00

Experimental Section

Cyt c_4 from *P. stutzeri* (ATCC No. 11607, DSM Braunschweig No. 50227) was isolated and purified as reported.[9−11] $A_{511}/A_{522} \approx 1.2$. Protein concentrations were determined from the absorbance at 551 nm.[11] UV/vis spectra were recorded on a Milton Roy 3000 diode array spectrophotometer. Cyt c_4 was diafiltrated (Amicon Models 8200, 180 mL, and 8010, 10 mL, YM3 Amicon membranes) to 0.01 or 0.1 M phosphate buffer, pH = 7.5. All other chemicals were analytical grade and solutions made up in Milli-Q water (Millipore).

Electrodes were prepared from graphite or gold disks (5 mm diameter, 1 mm thick) mounted with silver-loaded two-component epoxy (RS Components) on brass cylinders. The cylinder was cemented in a Teflon holder with two-component epoxy (Epoxylite 3151, resin and hardener). The electrode surface was polished with 1200, 2400, and 4000 grit silicon carbide paper (Dragon Fly) and with 20-fold diluted water suspension of 0.1 μm Al_2O_3, rinsed, and treated in an ultrasonic water bath.

Electrochemical measurements were performed with an Eco Chemie Autolab potentiostat equipped with an ECD low-current module, controlled by the General Purpose Eco Chemie version 3.2 Software. A two-component all-glass cell connected with a Luggin capillary, placed in a Cypress Systems Faraday cage was used. The counter electrode was a semicylindrical Pt gauze. The reference chamber held a Ag/AgCl/3 M KCl reference electrode (Metrohm), 210 mV vs SHE, inserted in a 0.1 M KCl salt bridge (Metrohm). The working solution, containing always initially fully oxidized cyt c_4, was blanketed for 30 min with wet argon before experiments. Freshly polished and sonicated gold electrodes were dipped for 6 min in ≈0.5 mM promoter/buffer solution followed by careful flush with pure buffer.

The simulated voltammograms were obtained by numerical solution of Fick's second law for each species, incorporating intramolecular ET for mechanism II (cf. below). The interfacial kinetics were treated in Butler−Volmer form. Usual dimensionless variables were used for concentrations, time (t), distance (x), and intramolecular (k_i, s^{-1}) and standard interfacial ET rate constants (k_s(i), cm s^{-1}): $a_i = [A_i]/C^\circ$, $\tau = t[F\nu/RT]^{-1}$, $y = x[F\nu/DRT]^{1/2}$, $\Lambda_s(i) = k_s(i)[DF\nu/RT]^{-1/2}$, and $\lambda_i = k_i[F\nu/RT]^{-1}$. $[A_i]$ is the concentration of the ith species, C° the total cyt c_4 concentration, D the diffusion coefficient, F Faraday's number, ν the scan rate, R the gas constant, and T the temperature. All simulations were carried out using the fully implicit scheme with expanding space grid described by Rudolph[25] and locally developed software, written in Turbo Pascal, and executed on a 486 personal computer. The parameter β describing the degree of exponential expansion was 0.75 and the dimensionless parameter $D^* = \Delta\tau/(\Delta y)^2 = 10^7$. Time steps corresponding to 2 mV/step were used throughout.

Results

Cyclic Voltammetry. *Cyclic Voltammetry at Unmodified Electrodes*. No electrochemical signals of cyt c_4 at unmodified *gold* electrodes could be detected. Figure 1 shows cyclic voltammograms of cyt c_4 at edge plane (EPG) and randomly oriented graphite (RPG) electrodes. Composite features, indicative of electrochemical activity of each heme are observed. The strong electrochemical features of the *negatively* charged metalloprotein at the *negatively* charged EPG electrode, at low ionic strength is interesting and suggests that specific orientation and local rather than overall protein charge is important. This would imply that intramolecular ET is coupled to interfacial ET.

Cyclic Voltammetry at Modified Gold Electrodes. Much better voltammetric resolution was achieved when the gold electrodes were modified with cystamine, 4,4′-bpySS and 3-PMHC. Figure 2 shows voltammograms at *high* ionic strength (0.1 M phosphate). The following are notable:

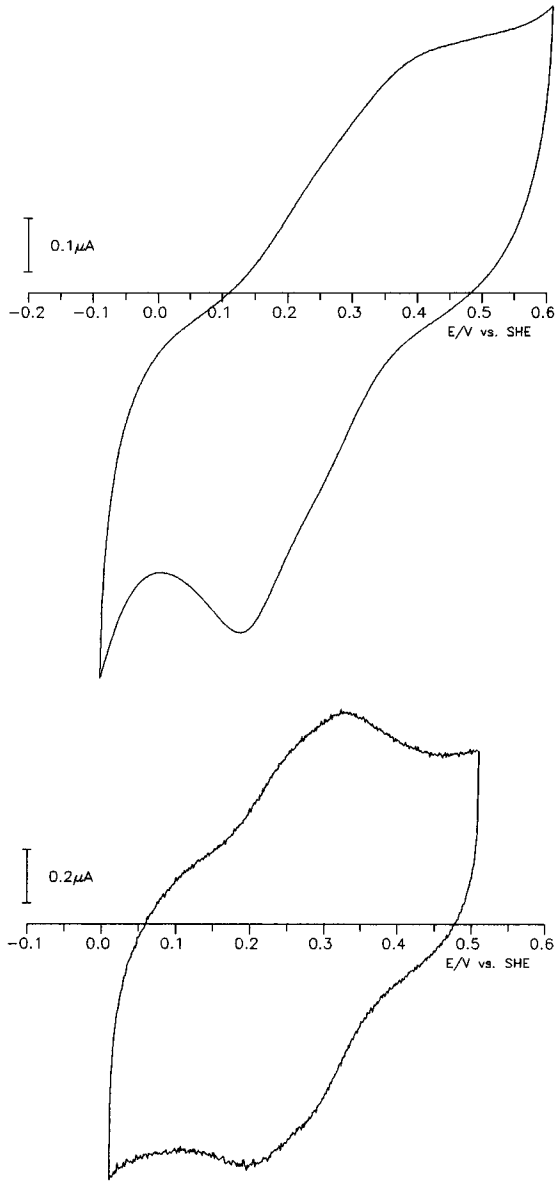

Figure 1. Voltammograms of cyt c_4 (75 μM) on EPG (top) and RPG (bottom). Scan rate 10 mV s^{-1}. Ag/AgCl/3 M KCl reference electrode. 0.01 M (EPG) and 0.1 M phosphate (RPG). pH 7.5.

(A) The cystamine- and 4,4′-bpySS-promoted voltammograms are stable. 3-PMHC gives stable voltammograms over a few scans followed by anodic peak deterioration.

(B) The voltammograms show clearly two peaks in *both* cathodic and anodic scans. From preliminary inspection the pair of cathodic and anodic peak separations are close to 59 mV. The composite features remain up to ≈200 mV s^{-1}. The average of the midpoint potentials is about 265 mV compared with 284 mV from ET kinetics in homogeneous solution.[9] Such differences are also encountered for other metalloproteins.[26] The reduction potentials can be resolved by numerical simulation, such as shown below.

(C) Quite similar voltammetric patterns on cystamine- and 4,4′-bpySS-modified gold electrodes are observed. This is very notable in view of the protein charge specificity commonly associated with these promoters.[23,24] This pattern can be referred to specific protein domain interaction with the promoter, and intramolecular ET in the time scale of the potential scans.

The voltammetric patterns are *different* and specific to the promoters at *low* ionic strength (0.01 M phosphate, Figure 3).

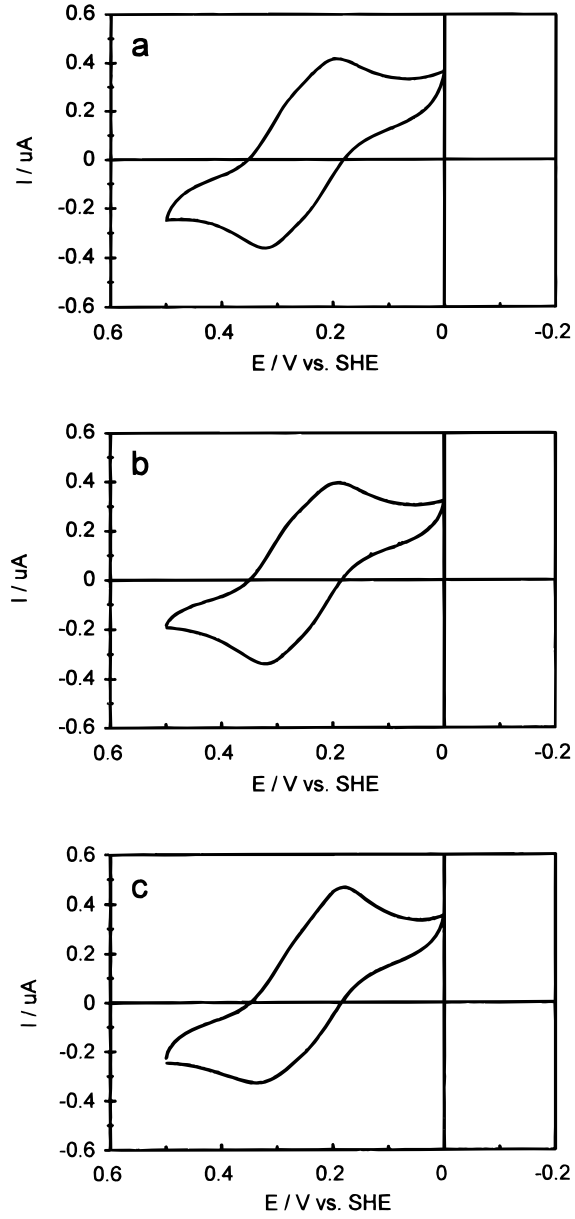

Figure 2. Cyclic voltammograms of cyt c_4 in 0.1 M phosphate (pH = 7.5), scan rate 10 mV s^{-1} on a gold electrode modified with (a) 3-PMHC, (b) 4,4′-bpySS, and (c) cystamine.

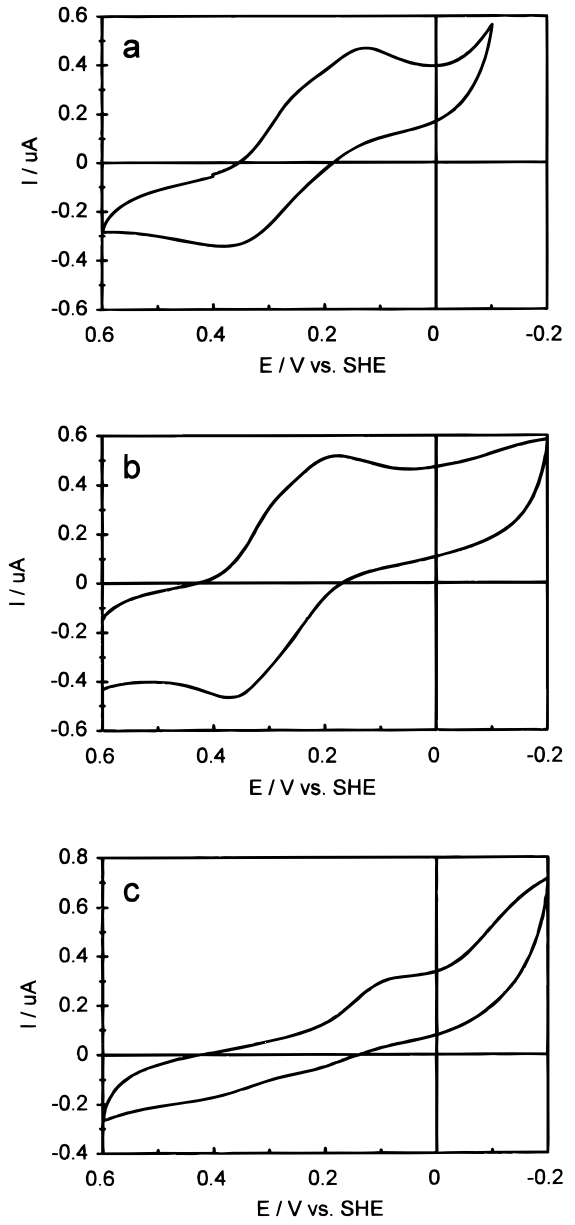

Figure 3. Cyclic voltammograms of cyt c_4 (75 μM) in 0.01 M phosphate (pH = 7.5), scan rate 10 mV s^{-1} on a gold electrode modified with (a) 3-PMHC, (b) 4,4′-bpySS, and (c) cystamine.

Observations here are as follows: (1) The anodic peaks at the cystamine-modified electrode are lower but better resolved than at high ionic strength. The cathodic peaks have merged into a single, two-electron peak. (2) A similar pattern appears for 4,4′-bpySS except that the cathodic peaks remain whereas the anodic signals have merged into a single peak. (3) The changes for 3-PMHC compared with high ionic strength are minor. Both peaks remain in each scan direction and instability appears on continued scanning.

Numerical Analysis. *Mechanistic Models for Cyt c_4 Voltammetry*. Two different mechanistic views of the cyt c_4 voltammetry, at both high and low ionic strength are formally consistent with the data:

Mechanism I: Cyt c_4 diffuses freely to the electrode and each heme group exchange electrons *exclusively* by interfacial ET, and at both high and low ionic strength, i.e.

$$A + e \rightleftarrows A^- \qquad k_s(1), E°(1) \tag{1}$$

$$A^- + e \rightleftarrows A^{2-} \qquad k_s(2), E°(2) \tag{2}$$

A represents fully oxidized and A^{2-} fully reduced cyt c_4. A^- is cyt c_4 with the high-potential heme group (center 1, in the positively charged C-terminal domain) reduced, and the low-potential heme group (center 2, in the negatively charged N-terminal domain) oxidized. $k_s(i)$ (i = 1, 2) is the interfacial ET rate constant and $E°(i)$ the reduction potentials.

Mechanism II: Interfacial ET of the heme groups with *parallel* intramolecular ET between the hemes. At low ionic strength, with rigid cyt c_4 orientation the scheme is

$$A + e \rightleftarrows A^- \qquad k_s(A), E°(A) \tag{3}$$

$$A^- \rightleftarrows B^- \qquad k_f, k_b \tag{4}$$

$$B^- + e \rightleftarrows A^{2-} \qquad k_s(A'), E°(A') \tag{5}$$

The notation is slightly more composite than in eqs 1 and 2. A is still fully oxidized and A^{2-} fully reduced cyt c_4. A^- is cyt c_4 with the *high*-potential heme (center 1) reduced and the *low*-potential heme (center 2) oxidized when 4,4′-bpySS is the promoter. B^- is the half-reduced cyt c_4 with the high-potential

heme oxidized and the low-potential heme reduced. The notation of A^- and B^- is opposite when cystamine is the promoter. $k_s(A)$ and $k_s(A')$ are interfacial ET rate constants, while $E°(A)$ and $E°(A')$ are the reduction potentials in eqs 3 and 5. In general $k_s(A) \neq k_s(A')$ and $E°(A) \neq E°(A')$ due to interactions between the heme groups, but this is disregarded in the following. Similar schemes, with less orientational selectivity and involving ET of both hemes, apply at high ionic strength.

Mechanism II holds the following intriguing perspective. The voltammetric appearance at *high* ionic strength implies that interfacial ET at either heme group occurs independently of the promoter. On the other hand, at *low* ionic strength the electrostatically dominated surface interaction orients cyt c_4 to match the promoter. Only the heme adjacent to the electrode is then engaged in direct interfacial ET, whereas the remote heme group is oxidized or reduced via intramolecular ET. Cyt c_4 is oriented at, say the 4,4′-bipySS-modified surface with the positively charged, high-potential domain toward the surface. As the potential is scanned cathodically, this heme is reduced first, followed by reduction of the remote heme (center 2) at a lower potential. The latter reduction is by intramolecular ET from the adjacent to the remote heme, followed by fast interfacial ET to the adjacent heme. The two steps occur at different potentials, giving two voltammetric peaks. As the scan is reversed, the oxidation potential of the low-potential heme is reached first. This group is, however, too remote for interfacial ET, which begins only when the oxidation potential of the adjacent, high-potential heme is reached. The ET sequence at the potential of this heme is then interfacial single-ET from the adjacent, high-potential heme, subsequent intramolecular ET from the remote low- to the adjacent high-potential heme, and a second interfacial single-ET from the adjacent high-potential heme. If intramolecular ET is fast on the time scale of the potential scan the anodic voltammogram appears as single interfacial two-ET.

A similar pattern is expected for cystamine except that the anodic peaks remain separated whereas the cathodic peaks coalesce into a single peak. 3-PMHC is less selective, and as for *all* the promoters at high ionic strength the voltammograms are rather a superposition of two interfacial single-ET peaks.

Determination of E° at High Ionic Strength. The experimental data at *high* ionic strength were stored and the first derivative obtained numerically using a 15-point Savitzky-Golay procedure.[27] The advantages of using the first derivative are (cf. Figure 4): (a) preciser determination of the potentials of the "shoulders", i.e., $E_p^{ox}(1)$ and $E_p^{red}(2)$, and (b) minimization of the peak potential shifts due to sloping baselines. The peak potentials were determined as in Figure 4b, i.e., $E_p^{red}(1)$ as the local minimum *before* the switch potential, $E_p^{red}(2)$ as the *intersection with* the baseline *before* the switch; $E_p^{ox}(2)$ as the local maximum *after* the switch potential, and $E_p^{ox}(1)$ as the *intersection* with the baseline after the switch. $E°$ was calculated as the midpoint potential, $E°(1) = {}^1/_2(E_p^{ox}(1) + E_p^{red}(1))$ and $E°(2) = {}^1/_2(E_p^{ox}(2) + E_p^{red}(2))$. However, it may be shown that the overlap of two closely spaced transitions causes a potential shift in *all* the peak potentials. $E_p^{red}(1)$ and $E_p^{ox}(1)$ are shifted *negative*, and $E_p^{red}(2)$ and $E_p^{ox}(2)$ *positive*, resulting in $E°$ shifts as indicated in Figure 4a. The "error" in $E°$ determined from the experimental data depends on the "real" $\Delta E°$ value and increases from ≈0 mV when $\Delta E° = 0.2$ V to ≈±14 mV when $\Delta E° = 0.08$ V. The peak separations $E_p^{ox}(1) - E_p^{red}(1)$ and $E_p^{ox}(2) - E_p^{red}(2)$ are little affected by the "overlap".

The $E°$ values at *high* ionic strength obtained after "overlap" correction are given in Table 1, which also includes the macroscopic $E°$ values from stopped-flow ET kinetics.[9,10] The potential separations for the individual peaks point to reversible behavior for both hemes and all the three promoters at high ionic strength, with slight negative $E°$ shifts (20−25 mV) compared with homogeneous solution. The data at *low* ionic strength are less straightforward due to slow interfacial ET and treated in the next subsection.

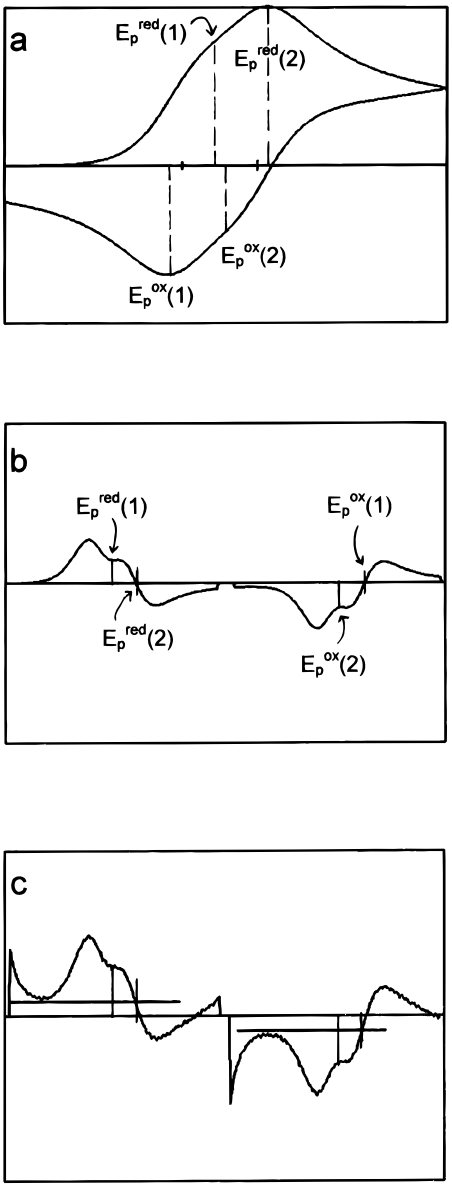

Figure 4. (a) Simulated voltammogram (mechanism I, $\Delta E° = 0.08$ V, $\Lambda_s(1) = \Lambda_s(2) = 100$). (b) The first derivative of the voltammogram in (a). (c) The first derivative voltammogram in Figure 2a including the baseline applied for determination of $E_p^{red}(2)$ and $E_p^{ox}(1)$.

TABLE 1: *E°*'s Determined as the Midpoint Potentials of the Reduction and Oxidation Peaks after Numerical Differentiation (Corrected for the Effect of Overlapping Peaks)[a] Compared with the *E°*'s Determined by Stopped-Flow Kinetic Investigations[b] of ET between Cyt c_4 and $[Co(bpy)_3]^{2+/3+}$ or $[Co(terpy)_2]^{2+/3+}$

promoter	$E°(1)$ (V vs SHE)	$E°(2)$ (V vs SHE)	$\Delta E°$ (mV)
3-PMHC	0.308	0.228	80
4,4′-bpySS	0.308	0.226	82
cystamine	0.308	0.224	84
hom kin[9]	0.328	0.241	87
hom kin[10]	0.330	0.256	74

[a] Based on voltammograms recorded at $\nu = 10$ mV s^{-1} with a cyt c_4 concentration of 75 μM and a phosphate buffer concentration of 0.1 M. [b] Assuming biexponential kinetics.

TABLE 2: Experimentally Determined $\Delta E_p(1)$, $\Delta E_p(2)$, and ΔE_p[a] from Voltammograms of Cyt c_4 (75 μM) at High (0.1 M) and Low (0.01 M) Buffer Concentrations Using the Three Promoters 3-PMHC, 4,4′-bpySS, and Cystamine

	[buff] = 0.1 M			[buff] = 0.01 M		
promoter	$\Delta E_p(1)$ (mV)	$\Delta E_p(2)$ (mV)	ΔE_p (mV)	$\Delta E_p(1)$ (mV)	$\Delta E_p(2)$ (mV)	ΔE_p (mV)
3-PMHC	57	61	108	104	102	173
4,4′-bpySS	57	60	109	144		224
cystamine	67	85	130		190	349

[a] $\Delta E_p(1) = E_p^{ox}(1) - E_p^{red}(1)$, $\Delta E_p(2) = E_p^{ox}(2) - E_p^{red}(2)$, and $\Delta E_p = E_p^{ox}(1) - E_p^{red}(2)$.

TABLE 3: $\Delta E_p(1)$, $\Delta E_p(2)$, and ΔE_p[a] Obtained from the Best Fit to Mechanism I at High and Low Buffer Concentrations As Described in the Text[b]

	[buff] = 0.1 M			[buff] = 0.01 M		
promoter	$\Delta E_p(1)$ (mV)	$\Delta E_p(2)$ (mV)	ΔE_p (mV)	$\Delta E_p(1)$ (mV)	$\Delta E_p(2)$ (mV)	ΔE_p (mV)
3-PMHC	61	60	113	101	104	171
4,4′-bpySS	61	63	114	140		241
cystamine	68	62	117		170	346

[a] $\Delta E_p(1) = E_p^{ox}(1) - E_p^{red}(1)$, $\Delta E_p(2) = E_p^{ox}(2) - E_p^{red}(2)$, and $\Delta E_p = E_p^{ox}(1) - E_p^{red}(2)$. [b] The corresponding values of $\Delta E°$ and the interfacial ET rate constants are given in Table 5.

TABLE 4: $\Delta E_p(1)$, $\Delta E_p(2)$, and ΔE_p[a] Obtained from the Best Fit to Mechanism II at High and Low Buffer Concentrations As Described in the Text[b]

	[buff] = 0.1 M			[buff] = 0.01 M		
promoter	$\Delta E_p(1)$ (mV)	$\Delta E_p(2)$ (mV)	ΔE_p (mV)	$\Delta E_p(1)$ (mV)	$\Delta E_p(2)$ (mV)	ΔE_p (mV)
3-PMHC	58	58	116	101	103	173
4,4′-bpySS	58	58	116	137		246
cystamine	65	74	120		198	342

[a] $\Delta E_p(1) = E_p^{ox}(1) - E_p^{red}(1)$, $\Delta E_p(2) = E_p^{ox}(2) - E_p^{red}(2)$, and $\Delta E_p = E_p^{ox}(1) - E_p^{red}(2)$. [b] The corresponding values of $\Delta E°$, interfacial ET rate constants and intramolecular ET rate constants are given in Table 6.

Rate Constants for Intramolecular and Interfacial ET. Three quantities were first extracted from *all* the data, using the first-derivative method, namely, $\Delta E_p(1) = E_p^{ox}(1) - E_p^{red}(1)$, $\Delta E_p(2) = E_p^{ox}(2) - E_p^{red}(2)$, and $\Delta E_p = E_p^{ox}(2) - E_p^{red}(1)$ (Table 2). The voltammograms were then analyzed based on mechanism I, assuming (a) $\Delta E°$ is independent of the promoter, and (b) the interfacial ET rate constants are attenuated by a common factor (also common for the promoters) on lowering the ionic strength. The assumptions are crude but keep the number of parameters small. The further strategy was as follows:

(1) The simulated voltammograms were first fitted to the data in Table 2 for *low* ionic strength and 3-PMHC by variation of $\Delta E°$ and $\Lambda_s(i)$. The resulting voltammetric parameters are given in Tables 3 and 5. $\Delta E°$ at *high* ionic strength (≈80 mV) is always smaller than the "best" value of 95 mV at *low* ionic strength.

(2) $\Delta E°$ was then fixed at 95 mV and fitting to the voltammograms at *low* ionic strength for 4,4′-bipySS and cystamine undertaken by varying $\Lambda_s(1)$ and $\Lambda_s(2)$ (Tables 3 and 5).

(3) The interfacial ET rate constants at *high* ionic strength were based on $\Delta E° = 80$ mV but since both interfacial ETs are here close to Nernstian, assumption (b) above was exploited. $\Lambda_s(1)$ and $\Lambda_s(2)$ in Table 5 are based on 100-fold increase from low to high ionic strength. Except for cystamine this gives simulated values of $\Delta E_p(1)$, $\Delta E_p(2)$, and ΔE_p (Table 3) in good agreement with the experimental data in Table 2. Larger $\Lambda_s(1)$ and smaller $\Lambda_s(2)$ at *high* ionic strength improves the agreement for cystamine.

TABLE 5: $\Delta E°$ and Dimensionless Interfacial ET Rate Constants, $\Lambda_s(1)$ and $\Lambda_s(2)$[a], Used To Obtain the Best Fit to Mechanism I at High and Low Buffer Concentrations As Described in the Text and Shown in Table 3

	[buff] = 0.1 M			[buff] = 0.01 M		
promoter	$\Delta E°$ (mV)	$\Lambda_s(1)$	$\Lambda_s(2)$	$\Delta E°$ (mV)	$\Lambda_s(1)$	$\Lambda_s(2)$
3-PMHC	80	100	100	95	1	1
4,4′-bpySS	80	60	20	95	0.6	0.2
cystamine	80	5	50	95	0.05	0.5

[a] $\Lambda_s(i) = k_s(i)\,[DF\nu/(RT)]^{-1/2}$, where $k_s(i)$ is the rate constant for the ith interfacial ET, D the diffusion coefficient of cyt c_4, and ν the scan rate.

The following assumptions were invoked in the analysis of *mechanism II*: (a) $\Delta E°$ is again independent of the promoter, and both cyt c_4 centers are electroactive toward *all* the promoters at *high* ionic strength *and* toward 3-PMHC at low ionic strength; (b) *only* center 1 (high-potential, positively charged) is electroactive for 4,4′-bpySS and *only* center 2 (low-potential, negatively charged) for cystamine at *low* ionic strength; (c) the intramolecular ET equilibrium constant is $K = \exp(F\Delta E°/RT)$, i.e., $K < 1$ when center 1, and $K > 1$ when center 2 is electroactive; (d) the intramolecular ET rates are independent of the promoter.

Further, (1) 3-PMHC at low ionic strength was examined first. Introducing intramolecular ET but assuming both centers to be electroactive affects the simulated voltammograms only weakly. The peaks are slightly sharpened, giving smaller $\Delta E_p(1)$, $\Delta E_p(2)$, and ΔE_p for the same $\Delta E°$, $\Lambda_s(1)$ and $\Lambda_s(2)$. Keeping $\Delta E° =$ 95 mV as for mechanism I gives $\Lambda_s(1) = \Lambda_s(2) = 0.9$ instead of $\Lambda_s(1) = \Lambda_s(2) = 1$ (Tables 4 and 6).

(2) Choosing $\Delta E° = 95$ mV for all the voltammograms at *low* ionic strength, the equilibrium constant for ET from the adjacent to the remote center is 0.025 for 4,4′-bipySS and 40 for cystamine. Variation of interfacial and intramolecular ET rate constants provides fits to the recorded voltammograms at low ionic strength for 4,4′-bpySS and cystamine. The resulting parameter values are given in Tables 5 and 6. The λ_i values (i = f, b) correspond to $k_i = 40\ s^{-1}$ for ET from center 1 (high potential) to center 2 (low potential) and $1600\ s^{-1}$ for ET in the opposite direction. Figure 5 illustrates the fits and the sensitivity of the voltammetric shapes to the intramolecular ET parameters.

(3) λ_f and λ_b were used in a simulation corresponding to 3-PMHC at low ionic strength to substantiate the initial step (point (1)).

(4) The same mechanism as for 3-PMHC at low ionic strength was used at high ionic strength for all the promoters, i.e., both centers being electroactive *in parallel* with intramolecular ET. $\Delta E°$ at high ionic strength is 80 mV, but intramolecular ET is here of little importance for the peak shapes and potentials since the interfacial ET rates are large. Keeping the intramolecular rate constant in the thermodynamically unfavored direction at the value from *low* ionic strength, using the voltammetric parameters in Table 6, and varying the interfacial ET rate constants give the values in Table 5.

Discussion

We have investigated the electrochemistry of negatively charged, dipolar two-domain cyt c_4 at gold electrodes modified with three different promoters. Well-behaved cyclic voltammograms were obtained in all cases. The voltammetric patterns were similar at high (0.1 M) ionic strength. This is notable since two of the promoters are known to be effective solely toward negatively (cystamine) or positively (4,4′-bpySS) charged single-center proteins.[23,24] Differences appear at low ionic

TABLE 6: $\Delta E°$, the Dimensionless Interfacial ET Rate Constants, $\Lambda_s(1)$ and $\Lambda_s(2)$[a], and the Dimensionless Intramolecular ET Rate Constants[b] Used To Obtain the "Best" Fit to Mechanism II at High and Low Buffer Concentrations As Described in the Text and Shown in Table 4

	[buff] = 0.1 M					[buff] = 0.01 M				
promoter	$\Delta E°$ (mV)	$\Lambda_s(1)$	$\Lambda_s(2)$	λ_f	λ_b	$\Delta E°$ (mV)	$\Lambda_s(1')$[c]	$\Lambda_s(2')$[c]	λ_f	λ_b
3-PMHC	80	90	90	100	2270	95	0.9	0.9	100	4040
4,4′-bpySS	−80	90	90	100	2270	−95	0.8	1	100	4040
cystamine	80	90	2	2270	100	95	0.35	0.35	4040	100

[a] $\Lambda_s(i) = k_s(i)[DF\nu/(RT)]^{-1/2}$, where $k_s(i)$ is the rate constant for the ith interfacial ET, D the diffusion coefficient of cyt c_4, and ν the scan rate. [b] $K = \lambda_f/\lambda_b = \exp[F\Delta E°/(RT)]$, and $\lambda_f = k_f[F\nu/(RT)]^{-1}$, $\lambda_b = k_b[F\nu/(RT)]^{-1}$, where $\Delta E° \equiv E°$(active center) $- E°$(inactive center) in the cases where 4,4′-bpySS and cystamine are promoters. [c] $\Lambda_s(1')$ and $\Lambda_s(2')$ represent the rate constant for interfacial ET to the two *different* redox centers in cyt c_4 in case of 3-PMHC, whereas $\Lambda_s(1')$ represents the interfacial ET rate constant to center(1) with center(2) in the oxidized form while $\Lambda_s(2')$ represents the rate constant to center(1) with center(2) in the reduced form in the case of 4,4′-bpySS. In the case of cystamine $\Lambda_s(1')$ represents the interfacial ET rate constant to center(2) with center(1) in the oxidized form while $\Lambda_s(2')$ represents the rate constant to center(2) with center(1) in the reduced form.

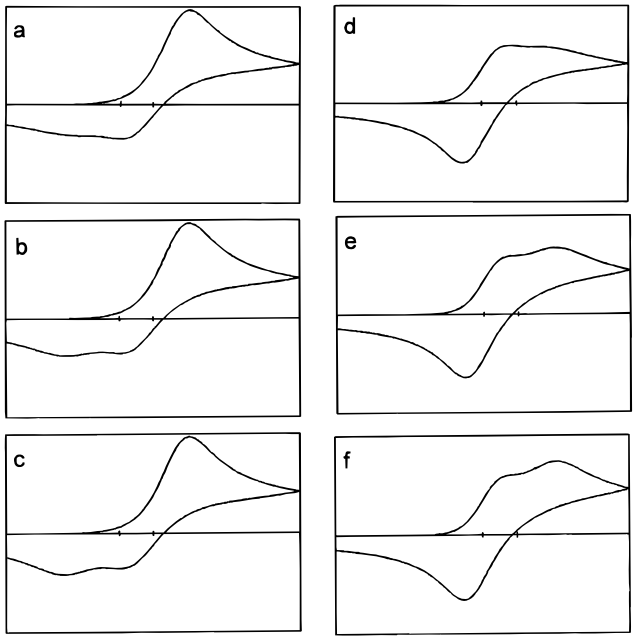

Figure 5. Sensitivity of mechanism II to the intramolecular ET rate constants. $\Delta E° = 0.095$ mV and potential range 0.8 V in all cases. (a) $K = 40$, $\Lambda_s(2) = \Lambda_s(2') = 0.35$, $\lambda_b = 10$. (b) $K = 30$, $\Lambda_s(2) = \Lambda_s(2') = 0.35$, $\lambda_b = 100$. (c) $K = 40$, $\Lambda_s(2) = \Lambda_s(2') = 0.35$, $\lambda_b = 1000$. (d) $K = 0.025$, $\Lambda_s(1) = 0.8$, $\Lambda_s(1') = 1$, $\lambda_f = 10$. (e) $K = 0.025$, $\Lambda_s(1) = 0.8$, $\Lambda_s(1') = 1$, $\lambda_f = 100$. (f) $K = 0.025$, $\Lambda_s(1) = 0.8$, $\Lambda_s(1') = 1$, $\lambda_f = 1000$. K is the equilibrium constant for intramolecular ET *from* the adjacent *to* the remote center. The simulated voltammograms can be compared with the experimental data in Figure 3.

strength. Lower ionic strength enhances the *anodic* peak resolution when cystamine is used, while the *cathodic* currents merge into a single peak. A reverse pattern arises for 4,4′-bpySS. Both electrostatic considerations and NMR and EPR spectroscopic data assign, importantly, the *low*-potential heme to the *negatively* and the *high*-potential heme to the *positively* charged domain.[9,10,22]

The voltammograms offer interesting implications for the protein−electrode surface interaction and for interfacial or intramolecular ET. The voltammograms at *high* ionic strength are indicative of little orientational selectivity and direct interfacial ET of both domains. This could be because the electrostatic screening is strong and protein charges are weakly conspicuous. The promoters, however, still seem to have an important role in preventing cyt c_4 from interacting directly with the gold surface as no electrochemical ET at unmodified gold electrodes was observed. This is supported by observations of drastic changes of reduction potential and other physical properties of cyt *c* on direct adsorption on gold and silver electrodes.[28,29] Another view might be that the protein is still oriented to match the promoters but the spatially remote domain directed toward the dielectrically screened surface. Such a pattern has been reported for the protein complex between Zn^{2+}-substituted cyt *c* (positively charged) and cyt b_5 (negatively charged).[30] This consideration is little affected by parallel intramolecular ET at high ionic strength.

$\Delta E°$ increases from 80 to 95 mV and the interfacial ET rate constants decrease by about 2 orders of magnitude when the buffer concentration is lowered from 0.1 to 0.01 M. The data at low ionic strength could concord *formally* with *mechanism I* by the following view. The low-potential interfacial rate constant ($k_s(2)$) is significantly smaller than the first, high-potential rate constant ($k_s(1)$) for 4,4′-bpySS, and vice versa for cystamine (Table 7). As cyt c_4 is reduced at, say 4,4′-bpySS, the second ET peak, $E_p^{red}(2)$ is therefore displaced more toward potentials negative of the equilibrium potential than the first peak, $E_p^{red}(1)$. This *increases* the cathodic peak separation compared with reversible behavior. The anodic peak potential, $E_p^{ox}(2)$ is similarly displaced more toward positive values than $E_p^{ox}(1)$, *decreasing* the anodic potential separation compared with the reversible limit. The cathodic peaks would thus remain separated at low ionic strength, but the anodic peak separation would narrow or vanish. A similar view, with the cathodic and anodic pattern reversed, applies to cystamine. This view and mechanism I do, however, give rather different values for the two remote heme rate constants (Table 7) and require a high degree of peak potential and rate constant matching. The implications of this are not obvious.

Mechanism II with more rigid cyt c_4 orientation at the lower ionic strength, applies more straightforwardly. Orientation would impede facile interfacial ET of the remote cyt c_4 domain, intramolecular ET being the only way in which this heme can be oxidized or reduced. The interfacial ET rate constants are also more consistent than for mechanism I, as seen by comparing $k_s(1)$ and $k_s(1')$ for 4,4′-bpySS, and $k_s(2)$ and $k_s(2')$ for cystamine (Table 7). The rate constants and midpoint potentials in Tables 6, 7, and 1 determined according to mechanism II call for the following further observations:

(a) The midpoint potential shifts at high ionic strength (Table 2) compared with homogeneous solution are small and could be associated with the different cyt c_4 environments (cf. ref 26).

(b) The smaller potential separation at high ionic strength is understandable from simple ionic screening. As ionic screening increases, the reduced state of the negatively charged low-potential domain is stabilized relative to the oxidized state, i.e., $E°(2)$ increases. The oxidized state of the positively charged high-potential domain is stabilized, lowering $E°(1)$.

(c) The interfacial ET rate constants drop by about 2 orders of magnitude when the buffer concentration is lowered from 0.1 to 0.01 M. This large effect would reflect a more constrained adsorption configuration, conformational changes,

TABLE 7: Interfacial ET Rate Constants Obtained from the Dimensionless Parameters Used in the "Best" Fit of the Voltammograms As Described in the Text[a]

	[buff] = 0.1 M		[buff] = 0.01 M		
promoter	$k_s(1)$[b] (cm s^{-1})	$k_s(2)$[b] (cm s^{-1})	$k_s(1)$[c] (cm s^{-1})	$k_s(2)$[d] (cm s^{-1})	$k_s(A')$[e] (cm s^{-1})
3-PMHC	$(3-6) \times 10^{-2}$	$(2-5) \times 10^{-2}$	$(5.6-6) \times 10^{-4}$	$(5.6-6) \times 10^{-4}$	
4,4′-bpySS	$(3-6) \times 10^{-2}$	$(2-5) \times 10^{-2}$	$(3.7-5) \times 10^{-4}$	1.2×10^{-4}	1.2×10^{-4}
cystamine	$(3-6) \times 10^{-2}$	$(0.1-0.3) \times 10^{-2}$	0.3×10^{-4}	$(2.2-3) \times 10^{-4}$	2.2×10^{-4}

[a] $k_s(i)$ calculated from $\Lambda_s(i) = k_s(i)[DF\nu/(RT)]^{-1/2}$ using $\nu = 10$ mV s^{-1} and $D = 10^{-6}$ cm^2 s^{-1}. [b] Derived from the dimensionless values in Tables 5 (mechanism **I**) and 6 (mechanism **II**). [c] For 3-PMHC and 4,4′-bpySS: using mechanism **I** and **II**, for cystamine: using mechanism **I**. [d] For 3-PMHC and cystamine: using mechanism **I** and **II**, for 4,4′-bpySS: using mechanism **I**. [e] For 4,4′-bpySS: reduction of center(1) after intramolecular ET to center(2), for cystamine: reduction of center(2) after intramolecular ET to center(1) (mechanism **II**).

or other perturbations of the cyt c_4 molecule caused by the stronger interaction with the modified surface at low ionic strength. Clues to the nature of these effects could be held by the approaches in refs 28 and 29.

An intriguing perspective relates finally to the *intra*molecular ET feature of mechanism II. Both interfacial and intramolecular ET rate constants at *high* ionic strength are quite inaccurate due to the almost Nernstian voltammetry. The intramolecular rate constants at *low* ionic strength are 40 (ET from high- to low-potential heme) and 1600 s^{-1} (low to high potential). In relation to the electronic properties[22] and multiexponential cyt c_4 ET kinetics in homogeneous solution[9,10,15] these values prompt the following observations:

(1) Considering the close proximity of the heme groups (19 Å center-to-center distance and hydrogen-bond contact through the propionates[21]), the rate constants appear *small*. NMR, resonance Raman, and low-temperature UV/vis spectroscopy[22] have, however, revealed pure low-spin reduced state and a temperature-dependent high-spin/low-spin equilibrium in the oxidized state. Such changes would be accompanied by significant structural changes. Together with the approximate thermoneutrality of the intramolecular process, this could easily lower the rate constants by many orders of magnitude compared to fast strongly exothermic ET of many modified hemoproteins.[31-33]

(2) The intramolecular ET rate constants can be compared to mechanistic conclusions in recent investigations of ET between cyt c_4 and the reaction partners $[Co(terpy)_2]^{2+/3+}$ (terpy = 2,2′,2″-terpyridine) and $[Co(bipy)_3]^{2+/3+}$ (bipy = 2,2′-bipyridine).[9,10] The kinetics here strongly suggest that *intra*molecular ET is either *fast* or *slow* compared with *inter*molecular ET, which is in the 10−100 ms range. The *intra*molecular process that would be part of the homogeneous ET schemes is dominated by the thermodynamically unfavored reaction, the voltammetrically determined value of which is ≈40 s^{-1}. This is in fact in a range similar to the *inter*molecular processes and should be detectable by the procedure in refs 9 and 10. This apparent contradiction must unfortunately be left open, but the ET rate constant of ≈40 s^{-1} could differ significantly from the value at high ionic strength and homogeneous environment used in refs 9 and 10. Corresponding work for lower ionic strength is in progress.

The overall conclusion is, then, that *both* cyt c_4 domains can be engaged in facile, almost reversible interfacial ET at *high* ionic strength. The data testify in favor of spatially constrained adsorption at *low* ionic strength where a detectable intramolecular ET channel opens.

Acknowledgment. Financial support from the Danish Natural Science Research Council and the EU Human Capital and Mobility Network, Activation of Organic Molecules by Electron Transfer, is acknowledged.

References and Notes

(1) Guo, L. H.; Hill, H. A. O. *Adv. Inorg. Chem.* **1991**, *36*, 341.
(2) Armstrong, F. A. *Struct. Bonding* **1990**, *72*, 137.
(3) Hill, H. A. O.; Hunt, N. I. *Methods Enzymol.* **1993**, *227*, 501.
(4) Armstrong, F. A.; Butt, J. N.; Sucheta, A. *Methods Enzymol.* **1993**, *227*, 479.
(5) Bogdanovskaya, V. A.; Tarasevich, M. *Sov. Sci. Rev. B Chem.* **1992**, *17*, 1.
(6) Yaropolov, A. I.; Gindilis, A. L. *Biofizika* **1990**, *35*, 689.
(7) Silvestrini, M. C.; Tordi, M. G.; Musci, G.; Brunori, M. *J. Biol. Chem.* **1990**, *265*, 11783.
(8) Schichman, S. A.; Meyer, T. E.; Gray, H. B. *Inorg. Chim. Acta* **1996**, *243*, 25.
(9) Conrad, L. S.; Karlsson, J.-J.; Ulstrup, J. *Eur. J. Biochem.* **1995**, *231*, 133.
(10) Karlsson, J.-J.; Rostrup, T. E.; Ulstrup, J. *Acta Chem. Scand.* **1996**, *50*, 284.
(11) Kodama, T.; Shirada, S. *J. Biochem. (Tokyo)* **1969**, *65*, 351.
(12) Swank, R. T.; Burris, R. H. *Biochim. Biophys. Acta* **1969**, *180*, 473.
(13) Hunter, D. J. B.; Brown, K. R.; Pettigrew, G. W. *Biochem. J.* **1989**, *262*, 233.
(14) Leitch, F. A.; Brown, K. R.; Pettigrew, G. W. *Biochim. Biophys. Acta* **1985**, *808*, 213.
(15) Gadsby, P. M. A.; Hartskorn, R. T.; Moura, J. J. G.; Sinclair-Day, J. D.; Sykes, A. G.; Thomson, A. J. *Biochim. Biophys. Acta* **1988**, *994*, 37.
(16) Moore, G. R.; Pettigrew, G. W. *Cytochromes c. Evolutionary, Structural and Physicochemical Aspects*; Springer-Verlag: New York, 1990.
(17) Myer, Y. P. *Curr. Top. Bioenerg.* **1985**, *14*, 149.
(18) For overviews, see refs 9, 13, 15, and 17.
(19) Christensen, H. E. M. *Gene* **1994**, *144*, 139.
(20) Christensen, H. E. M.; Kadziola, A.; Karlsson, J.-J.; Larsen, S.; Ulstrup, J. *Acta Crystallogr., Sect. D* **1995**, *51*, 1071.
(21) Kadziola, A.; Larsen, S. *Structure*, in press.
(22) Andersen, N. H.; Coutinho, I. B.; Karlsson, J.-J.; Nissum, M.; Smulevich, G.; Ulstrup, J.; Xavier, A. V., in preparation.
(23) Hill, H. A. O.; Page, D. J.; Walton, N. J.; Whitford, D. *J. Electroanal. Chem.* **1985**, *187*, 315.
(24) Hill, H. A. O.; Lawrence, G. A. *J. Electroanal. Chem.* **1989**, *270*, 309.
(25) Rudolph, M. *J. Electroanal. Chem.* **1991**, *314*, 13.
(26) Song, S.; Clark, R. A.; Bowden, E. F.; Taylor, M. J. *J. Phys. Chem.* **1993**, *97*, 6565.
(27) Savitzky, A.; Golay, M. J. E. *Anal. Chem.* **1964**, *36*, 1627.
(28) Hobara, D.; Niki, K.; Zhou, C.; Chumanov, G.; Cotton, T. M. *Colloid Interfaces A: Physicochem. Eng. Asp.* **1994**, *93*, 241.
(29) Hildebrandt, P.; Stockburger, M. *Biochemistry* **1989**, *28*, 6710.
(30) Barker, P. D.; Guo, L.-H., Hill, H. A. O.; Sanghera, G. S. *Biochem. Soc. Trans.* **1988**, *16*, 957.
(31) Gray, H. B.; Winkler, J. R. *Chem. Rev.* **1992**, *92*, 369.
(32) Scott, J. R.; Willie, A.; McLean, M.; Stayton, P. S.; Sligar, S. G.; Durham, B.; Millett, F. *J. Am. Chem. Soc.* **1993**, *115*, 6820.
(33) Mines, G. A.; Bjerrum, M. J.; Hill, M. G.; Casimiro, D. R.; Chang, I.-J.; Winkler, J. R.; Gray, H. B. *J. Am. Chem. Soc.* **1996**, *118*, 1961.